Desalination and Water Treatment
www.deswater.com

22 (2010) 146–155
October

doi: 10/5004/dwt.2010.1390

The biosorption of Safranine onto *Parthenium hysterophorus* L: Equilibrium and kinetics investigation

V.S. Shrivastava

Department of P.G. Studies and Research in Chemistry, G.T.P. College, Nandurbar 425412, Maharashtra, India
Tel. +91 2564 234248; email: drvinod_shrivastava@yahoo.com

Received 28 November 2009; Accepted 6 April 2010

ABSTRACT

The effectiveness of adsorption for dye removal from wastewater has made it an ideal alternative to other expensive treatment options. The removal of Safranine onto *Parthenium hysterophorus* L (congress grass) (CG) from aqueous solutions was investigated using parameters such as contact time, pH, adsorbent doses, and initial dye concentration. Adsorption isotherms of dye onto CG were determined and correlated with common isotherm equations such as the Langmuir and Freundlich model. Adsorption equilibrium was reached within 40 min. Parameters of the Langmuir and Freundlich isotherms were determined using adsorption data. The maximum adsorption capacity of Safranine onto CG was found to be 89.3 mg/g at 400 mg/l of dye concentration. The equilibrium data satisfied Langmuir isotherm better than Freundlich isotherm. The rate constants were evaluated for initial dye concentration and adsorbent doses. The experimental data fit the pseudo-second-order kinetic model.

Keywords: Adsorption; Isotherms; Kinetics; Safranine; *Parthenium hysterophorus*; XRD

1. Introduction

The textile dyeing industry consumes large quantities of water at its different steps of dyeing and finishing processes. Due to the large volumes of water consumption, the production of huge volume of wastewater is inevitable [1]. Textile dyeing—printing industry wastewater is highly charged with consumed dyes, surfactants and sometimes traces of metals. It is estimated that 1–15% of the dye is lost during dyeing section of a textile industry process and is released in wastewaters [2]. These effluents cause a lot of damage to the environment. In most countries researchers are looking for appropriate treatments in order to remove pollutants, impuritiesand decolorization of dye house effluents [3–5]. Due to more and more increasingly stringent restrictions on the hazardous organic content of industrial effluents it is necessary to eliminate organic pollutants by proper treatment methods before being released it into the water courses [6]. Various techniques such as adsorption [7], nanophotocatalysis [8], electrochemical [9], membrane processes [10], etc. have been used for the removal of organics as well as inoragnics from wastewaters. The non-degradable nature of dyes and their stability towards light and oxidizing agents complicate the selection of suitable method for their removal. In comparisons to the removal methods of colors, it has been well established that adsorption is the most convenient and effective. Various chemical and physical processes are currently used, which work by direct precipitation and separation of pollutants [11] or elimination by adsorption on activated carbon or similar materials. It is well known that liquid-phase adsorption is one of the most efficient methods for removal of colors, odors and organic pollutants from process or waste effluents. In addition, activated carbons are the most widely used adsorbents because of their excellent adsorption ability for relatively low molecular weight

organic matters. However, their use is usually limited due to its high cost [11–14]. These lead many workers to search for cheaper subsistent including fly ash [15], coal, silica gel, wool waste and clay materials [6], have been applied with varying success for removal of color and metals. Of these alternatives, many agricultural and wood wastes such as cane (bagasse) pith [16], maize cob [17], sawdust [18], fruit kernels, coconut husk, fibers and bittim shells [19], wheat shell [20], neem leaf powder [21], appear to be more economically attractive because they are abundant.

New economically, easily available and highly effective adsorbent are still needed. Parthenium (*Parthenium hysterophorus* L.) also known as congress grass, white top or carrot weed, an annual herbaceous weed—a native of North-east Mexico, has now widely spread in India, China, Australia, Pacific Islands, etc. The biomass of this plant is not put to any use and disposed along the road-sides, agricultural fields, and railway tracks after uprooting. The biomass of this plant is available round the year at zero prices.

In our laboratory, the work is in progress to look into the possibility of the use of waste biomass for industrial pollution control. The aim of the present work was to study the adsorption capacity of differential treated white top Parthenium plant for dye removal, Safranine, from aqueous solution under different experimental conditions and adsorption kinetics. The basic dyes are one of the most important and widely used dye groups in the textile dyeing industries. However, only a limited number of studies on Safranine removal were found in literature [22,23]. As Safranine is water soluble dye thus difficult to remove by common chemical treatment methods. Keeping this in mind it necessitates an attempt to find and provide an easy, feasible and reliable method for the removal, thus utilization of adsorption technique seems to be more fruitful. The focus of this investigation is to evaluate the adsorption potential of removal of Safranine. In this respect Safranine was used as model compound. The aim of the present study is to optimize the conditions for the maximum removal of Safranine on CG from aqueous solution. The effects of contact time, pH, dye concentration, adsorbent dose on the adsorption of Safranine onto CG were investigated. The Langmuir and Freundlich isotherms were used to fit equilibrium data. The pseudo-first-order, pseudo second-order, Elovich and intraparticle diffusion kineics models were attempted.

2. Materials and methods

2.1. Adsorbent material

Parthenium hysterophorus L (congress grass) (CG) was abundant available grass in Indian agricultural fields. The CG was collected from nearby agricultural fields, washed with double distilled water to remove adhering dirt, dried in sunlight, crushed and sieved through 60–250 μm size. This ground material was soaked for 18 h and washed with hot and cold distilled water, till the wash water is colorless. This washed material was then dried in oven at 50°C for 12 h and preserved in glass bottle for use as an adsorbent without any pretreatment.

2.2. Adsorbate

The basic dye Safranine was used in the study. Safranine was (C.I. = 50,240, chemical formula $C_{20}H_{19}N_4Cl$, MW = 350.5 g/mol, nature — basic dye, λ_{max} = 532 nm) supplied by S.D. Fine Chemicals, Mumbai of commercial purity were used without further purification. The structure of Safranine was given in Fig. 1. The dye stock solution was prepared by dissolving accurately weighed dye in distilled water to the concentration of 2000 mg/l. The experimental solutions were obtained by diluting the dye stock solution in accurate proportion to needed initial concentration.

2.3. Experimental methods and measurement

The adsorption experiments were carried out in a batch process at 30 °C by using aqueous solution of Safranine. In each experiment an accurately weighed amount of CG was added to 50 ml of the dye solution in 100 ml stoppard bottles and mixture was agitated on a mechanical shaker at a given time at constant temperature of 30 °C. The adsorbent was separated from solution by centrifugation. The absorbance of the supernatant solution was estimated to determine the residual dye concentration. The residual dye concentration was determined at lmax 532 nm with UV—visible spectrophotometer (Systronics 118). The experiments were carried out at initial pH values ranging from 2 to 11; initial pH was controlled by addition of 0.1 N HCl and 0.1 N NaOH solutions. Kinetics of adsorption was determined by analyzing adsorptive uptake of dye from aqueous solution at different time intervals. The X-ray diffraction (XRD), scanning electron microscope (SEM), Brunauer—Emmett—Teller (BET) and electron dispersion X-ray (EDX) element analysis of adsorbent was also carried out.

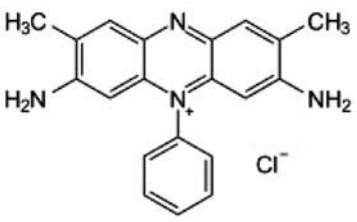

Fig. 1. The structure of Safranine.

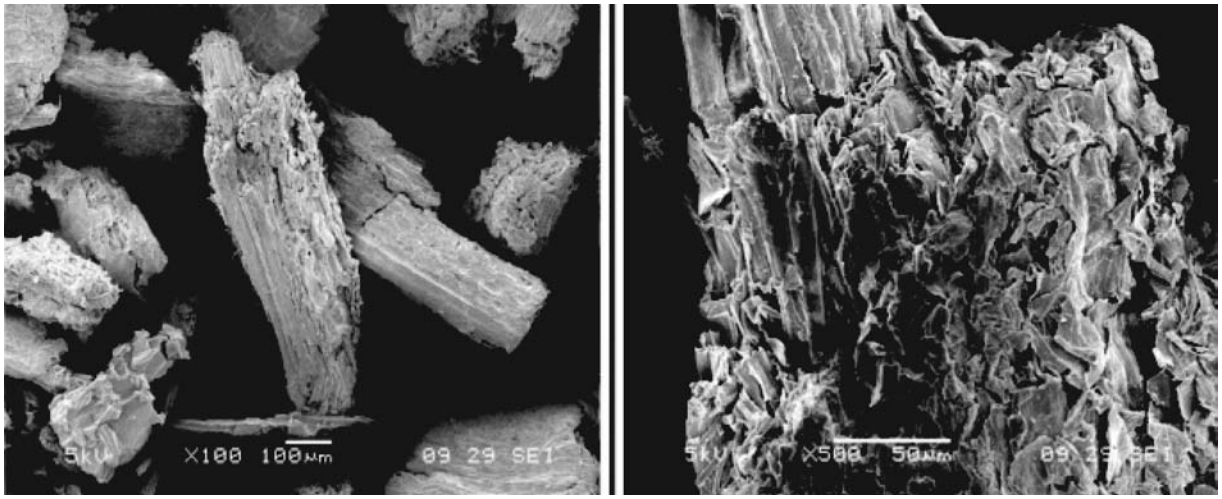

Fig. 2. The SEM micrographs of CG and CG dyed by Safranine.

3. Results and discussion

3.1. Adsorbent characterization

For structural and morphological characteristics XRD, SEM, BET and EDX of CG were carried out.

3.1.1. SEM and BET analysis

The SEM micrographs of CG and CG dyed with Safranine are shown in Fig. 2. As it is known, SEM is one of the most widely used surface diagnostic tools. The SEM micrographs of adsorbent CG and CG dyed with Safranine were carried out at different magnifications to know surface structure and porosity. CG has heterogeneous surface and micropores where there is a good possibility for dye to be trapped and adsorbed.

The BET surface area was found to be 19.28 m^2/g, Langmuir surface area 18.31 m^2/g, micropore area 0.89 m^2/g, mesopore area 173.41 m^2/g, micropore volume 0.0009 cm^2/g , mesopore volume 17.2 cm^3/g, mean pore diameter 6.48 Å and mean mesopore diameter 284.92 Å.

3.1.2. XRD and EDX analysis

Crystallinity of CG was determined by X-ray diffraction using diffractometer (D-8, Advance Bruker axs Germany using Cu-anode). The XRD diagram of adsorbent CG is shown in Fig. 3. The XRD pattern of raw adsorbent showed typical spectrum with main and secondary peak at 22.3° and 16.4°, respectively. The main peak is taken as indicative of the presence of highly organized crystalline cellulose while secondary peak is a measure of a less organized polysaccharide structure. The EDX analysis of CG shows the presence of 46.3% C, 38.2% O with mineral composition 0.36% Na, 0.28% Mg, 1.84% Al, 3.05% Si, 8.02% K and 1.95% Ca.

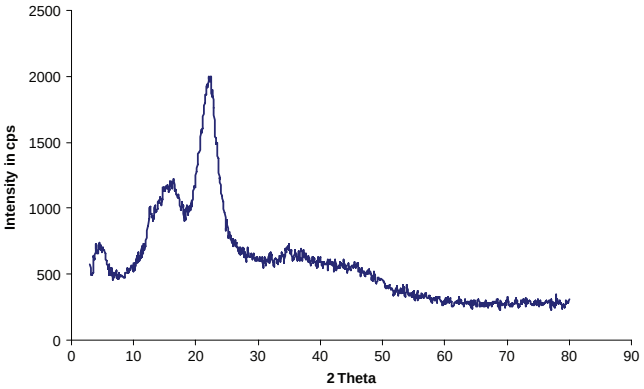

Fig. 3. The XRD diagram of CG adsorbent.

3.1.3. FTIR analysis

In order to investigate the surface characteristics of CG, Fourier transform infrared (FTIR) in the range 450–4000 cm^{-1} was studied. The FTIR spectrum of CG shows that the peak positions are at 3334.7, 2891.1, 1735, 1600.8, 1326.9 and 894.4 cm^{-1}. The bands at 3334.7 are due to O–H and N–H stretching. While the bands at 2891.1 and 1735 reflects C–CH_3 and –CO–O stretching, respectively. Bands at 1600.8 and 1326.9 corresponds to aromatic >C=C< and O–H bending, respectively while band at 894.9 cm^{-1} corresponds to $R_2C{=}CH_2$. Some of the groups shifted to lower frequency after adsorption are from 3334.7 to 3331, 1735 to 1730, 1600.8 to 1585 and 1326.9 to 1321 suggesting the participation of these groups in the adsorption of Safranine. This also suggests that adsorption of Safranine on CG is chemical adsorption.

3.2. Effect of pH

The pH of the dye solution plays an important role in the whole adsorption process and particularly on the adsorption capacity [19]. The adsorption of charged dye groups onto the adsorbent surface is primarily influenced by the surface charges on the adsorbent which is in turn influenced by the solution pH. The FTIR analysis showed that the CG contains large number of active sites and the solute uptake can be related to the active sites and also to the chemistry of the solute in the solution. The effect of initial pH on equilibrium capacity of CG was studied at 100 mg/l initial Safranine concentration, at contact time 40 min, with 4 g/l of CG at 30 °C. It shows that the sorption of Safranine was minimum 21% at initial pH 2 and increased with pH up to 6 (72%) and thereafter decreases to 51% at pH 11. The observed low adsorption capacity of Safranine on the CG at pH < 6 may be the surface charge become positively charged, thus making (H^+) ions compete effectively with dye cations causing a decrease in the amount of dye adsorbed. At high pH, the surface charge may get negatively charged which does not favors the adsorption of dye ions hence adsorption decrease to 51% at pH 11.

3.3. Effect of contact time and initial dye concentration

A series of experiments were performed to optimize the adsorption time at an initial dye concentration of 100, 200, 300 and 500 mg/l. with adsorbent dose of 2, 4 and 6 g/l. The results for effect of initial concentration and contact time on adsorption of Safranine onto CG at 30 °C are shown in Fig. 4. It was observed that dye uptake was rapid for the first 25 min, and thereafter proceeds at slower rate and finally attains saturation. This was caused by strong attractive forces between the dye molecules and the adsorbent; fast diffusion onto the external surface was followed by fast pore diffusion into the intraparticle matrix to attain rapid equilibrium. As the initial Safranine concentration increased from 100 to 500 mg/l the equilibrium removal of Safranine decreased from 82% to 65% (Fig. 4). The equilibrium adsorption increases from 40.9 to 161.7 mg/g with increase in initial Safranine concentration from 100 to 500 mg/l with 2 g/l of CG dose. Fig. 5 indicates that an increase in initial Safranine concentration leads to increase in the adsorption (q_e) of Safranine on CG.

The adsorption of Safranine on CG was found to reach equilibrium at 40 min for the concentration range studied (100–500 mg/l). However, the experimental data was measured up at 70 min to be sure that full equilibrium was attained. The variables like adsorbent dosage, pH and agitation speed was same for different experimental runs. The dye concentration affects the diffusion of dye molecules through the solution to the surface of the adsorbent. Higher concentration resulted in higher driving force of the concentration gradient. This driving force accelerated the diffusion of dye from solution into the adsorbent [18]. It is clear that the efficiency of dye removal depends on the initial dye concentration. The amount of dye adsorbed increases with increasing dye concentration and remained nearly constant after equilibrium time.

3.4. Effect of adsorbent dosage

An adsorbent dose is an important parameter because this determines the capacity of an adsorbent for a given initial concentration of adsorbate. The effect of adsorbent

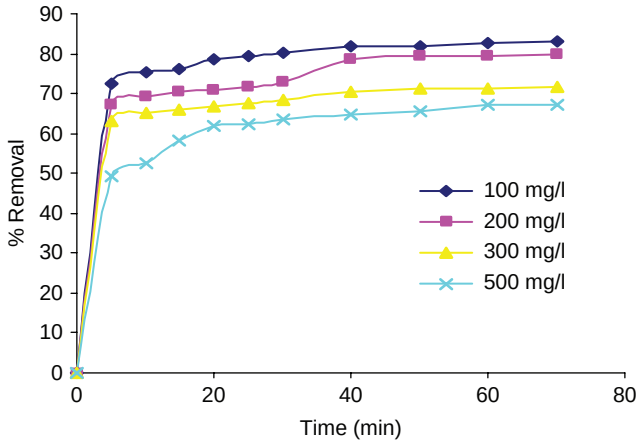

Fig. 4. Effect of contact time and concentration of Safranine on percent removal; adsorbent dose 2 g/l, pH 6.

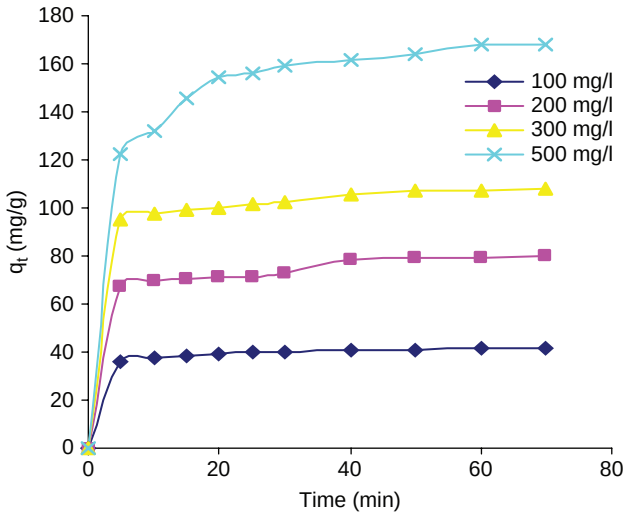

Fig. 5. Amount of dye adsorbed q_t (mg/g) with time (min) for different initial dye concentrations; adsorbent dose 2 g/l, pH 6.

doses was studied on dye removal, keeping all other experimental conditions constant. In order to investigate the effect of CG on Safranine adsorption, experiments were conducted at initial dye concentration of 100, 200, 300 mg/l with adsorbent dose from 1 to 12 g/l at pH 6 and contact time 40 min. Fig. 6 shows the effect of adsorbent dose on the amount of dye adsorption. The amount of dye adsorption (q_t) increases from 82 to 222 mg/g when the dye concentration increases from 100 to 300 mg/l at an adsorbent dose of 1 g/l. As adsorbent dose was increased from 1 to 12 g/l, the amount of dye adsorbed per unit mass of adsorbent (mg/g) decreases from 222 to 23 mg/g at a dye concentration of 300 mg/l, while percent removal was increased from 74% to 91%. The results show that as the adsorbent mass increases, the overall percentage of dye adsorbed also increases, but the amount adsorbed per unit mass of adsorbent decreases considerably. The increase in percent removal was due to the increase in the available sorption surface and sites. The decrease in unit adsorption with increase in the dose of adsorbent is basically due to adsorption sites remaining unsaturated during the adsorption process.

3.5. Adsorption kinetics

Adsorption is a physiochemical process that involves the mass transfer of solute (adsorbate) from the fluid phase to the adsorbent surface. A study of kinetics of adsorption is desirable as it provides information about the mechanism of adsorption, which is important for efficiency of the process [19]. The transient behavior of the dye adsorption process was analyzed by using pseudo-first order, pseudo-second order, Elovich and intraparticle diffusion.

3.5.1. Pseudo-first-order model

A linear form of pseudo-first-order equation was described by Lagergren [24].

$$\log(q_e - q_t) = \log q_e - \frac{K_1 t}{2.303} \quad (1)$$

where q_t and q_e are the amount of dye adsorbed (mg/g) at time t and at equilibrium, respectively. K_1 is the equilibrium rate constant of pseudo-first-order kinetics (min^{-1}). The straight line plots of log ($q_e - q_t$) versus t (Fig. 7) for the adsorption of Safranine onto CG at different initial dye concentrations (100–500 mg/l) and adsorbent dose 2–6 g/l have also been tested to obtain rate parameters. The rate constant observed was $2.51 \times 10^{-2} - 12.827 \times 10^{-2}$ min^{-1} (Table 1). The K_1, q_e calculated and correlation coefficients at adsorbent dose and dye concentration studied where calculated from these plots and are given in Table 1. The correlation coefficients r^2 listed in Table 1 for first-order kinetic model were ≥ 0.9262.

3.5.2. Pseudosecond-order equation

Data was applied to the Ho and McKay's pseudo-second-order chemisorptions kinetic rate equation which is expressed as [25,26].

$$\frac{t}{q_t} = \frac{1}{K_2 q_e^2} + \frac{t}{q_e} \quad \text{and} \quad h = K_2 q_e^2 \quad (2)$$

where K_2 is the rate constant of pseudo-second-order adsorption (g $mg^{-1}min^{-1}$). To understand the applicability

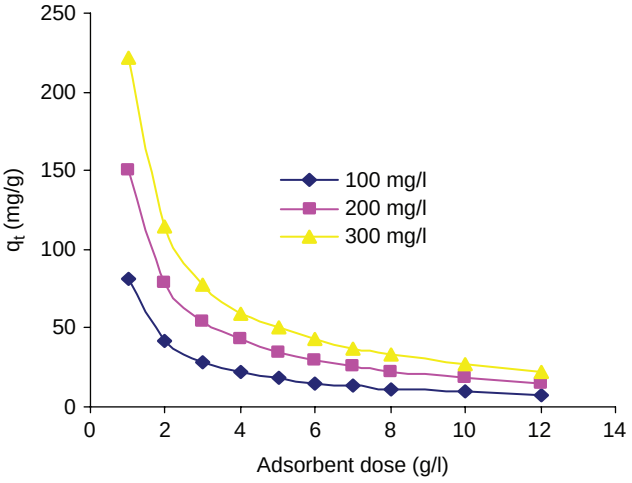

Fig. 6. Amount of dye adsorbed q_t (mg/g) with adsorbent dose (g/l) for different initial dye concentrations, contact time 40 min, pH 6.

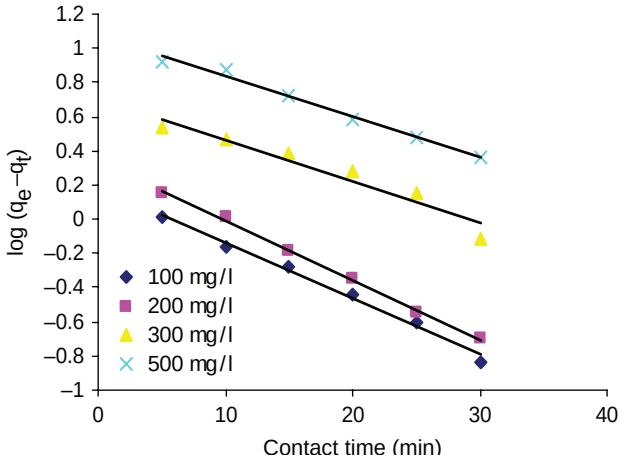

Fig. 7. First-order kinetic plots for the removal of Safranine at different initial dye concentrations; adsorbent dose 6 g/l, pH 6.

Table 1
Comparison of adsorption rate constants, calculated and experimental q_e values for different initial dye concentrations and adsorbent dose for different kinetic models for Safranine–CG

Adsorbent, g/l	Dye concentration, mg/l	Pseudofirst order				
		q_e (exp), mg/g	$K_1 \times 10^{-2}$, min^{-1}	q_e (cal), mg/g	r^2	
2	100	40.90	7.162	7.12	0.9864	
	200	78.41	2.510	12.20	0.9649	
	300	105.46	5.066	13.66	0.9941	
	500	161.65	7.139	7.12	0.9864	
4	100	21.60	5.941	1.80	0.9911	
	200	42.04	10.662	10.69	0.9821	
	300	62.50	7.277	14.55	0.9621	
	500	100.62	12.827	39.70	0.9578	
6	100	15.03	7.553	1.56	0.9916	
	200	29.06	8.037	2.20	0.9977	
	300	43.92	5.642	5.14	0.9262	
	500	71.97	5.481	11.83	0.9860	
		Pseudosecond order				
		$K_2 \times 10^{-3}$ g/mg min	q_e (cal), mg/g	t½	h	r^2
2	100	42.19	17.60	1.3465	31.35	0.9999
	200	82.64	9.72	1.2446	66.41	0.9982
	300	109.89	6.01	1.5166	72.46	0.9997
	500	175.43	2.98	1.9082	91.74	0.9996
4	100	22.32	44.80	0.9999	22.32	0.9998
	200	44.64	11.61	1.9285	23.15	0.9995
	300	64.51	9.07	1.7096	37.74	0.9998
	500	106.38	4.88	1.9258	55.25	0.9996
6	100	15.33	81.91	0.7959	19.27	0.9999
	200	29.49	30.73	1.1032	26.74	0.9999
	300	45.45	17.22	1.2774	35.59	0.9998
	500	73.53	10.22	1.3309	55.25	0.9998

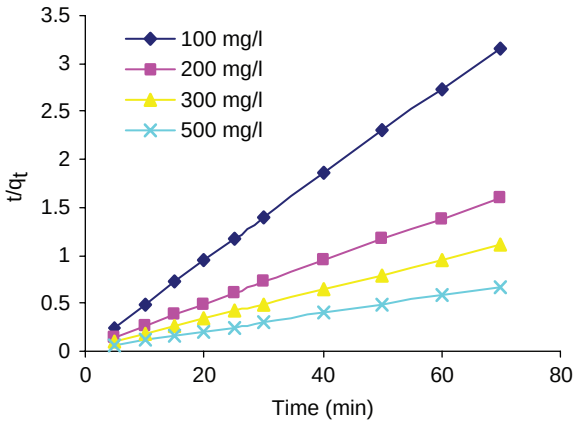

Fig. 8. Second-order kinetic plots for the removal of Safranine at different initial dye concentrations; adsorbent dose 4 g/l, pH 6.

of the model a linear plots of t/q_t versus t for different dye concentration (100–500 mg/l) with adsorbent dose (2–6 g/l) have been plotted are shown in Fig. 8. The K_2, q_e and correlation coefficients were calculated from these plots are given in Table 1. The rates of sorption were found to confirm to pseudo-second-order kinetics with good correlation $r^2 \geq 0.9982$ (Table 1). The q_e calculated values and q_e experimental also shows good agreement for pseudo-second-order kinetics than pseudo-first order.

3.5.3. The Elovich equation

The Elovich equation is given as follows [15]:

$$q_t = \frac{1}{\beta}\ln(\alpha\beta) + \frac{1}{\beta}\ln t \quad (3)$$

where α is the initial adsorption rate (mg g^{-1} min^{-1}), β is the desorption constant (g/mg) were calculated from intercept and slope of the straight line plot of q_t versus $\ln t$. It has been observed from the data that value of α and β varied as a function of initial dye concentration. Thus on increasing initial dye concentration from 100 to 500 mg/l, the value of β decreases from 0.4720 to 0.0557 g/mg for 2 g/l of adsorbent dose. The value

Table 2
Adsorption kinetic parameters of Safranine onto CG for Elovich and Intra-particle diffusion models

Adsorbent, g/l	Dye concentration, mg/g	Elovich model		Intraparticle diffusion	
		β, g/mg	r^2	K_p, mg/g/min$^{0.5}$	r^2
2	100	0.4720	0.9870	0.8586	0.9356
	200	0.1815	0.8812	2.3614	0.9342
	300	0.1762	0.9726	2.2014	0.9767
	500	0.0557	0.9586	7.1328	0.8726
4	100	1.3993	0.9704	0.2979	0.9720
	200	0.3416	0.9730	1.1941	0.9337
	300	0.2382	0.9437	1.7043	0.8970
	500	0.1324	0.9509	3.0361	0.8860
6	100	2.1372	0.9957	0.1898	0.9446
	200	1.5561	0.9758	0.2572	0.9018
	300	0.5554	0.9533	0.7591	0.9733
	500	0.2676	0.9521	1.5233	0.9129

of β increases from 0.4720 to 2.1372 g/mg as adsorbent dose was increased from 2 to 6 g/l for 100 mg/l of dye concentration (Table 2).

3.5.4. The intraparticle diffusion model

In order to investigate the mechanism of dye adsorption onto CG, intraparticle based mechanism was studied. The most commonly used technique for identifying the mechanism involved in the adsorption process is by fitting intraparticle diffusion plot. It is an empirically found functional relationship, common to most adsorption processes, where uptake varies almost proportionally with $t^{1/2}$ rather than with the contact time t. According to the theory proposed by Weber and Morris [27] the equation is;

$$q_t = K_p t^{1/2} + C \quad (4)$$

where K_p is the rate parameter of stage I (mg/g min$^{0.5}$), is obtained from the slope of the straight line of q_t versus $t^{1/2}$, whereas C is the intercept of the plot which gives an idea about the thickness of boundary layer. If intraparticle diffusion occurs, then q_t versus $t^{1/2}$ will be linear and if the plot passes through the origin, then the rate limiting process is only due to intraparticle diffusion. Otherwise, some other mechanism along with intraparticle diffusion is also involved [28]. The plots of q_t verses $t^{1/2}$ intraparticle diffusion model shown in Fig. 9 were not linear over the whole time range, implying that more than one process affected the adsorption. Such finding is similar to that made in previous works on adsorption [29]. These plots have a similar general trend with an initial curved part, followed by a linear one and then a plateau. The initial curved part may be attributed to the bulk diffusion, the linear one to the intraparticle diffusion and plateau to the equilibrium. This indicate that the

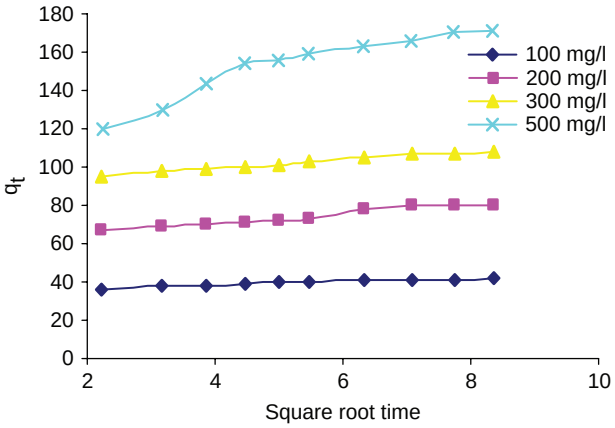

Fig. 9. Weber–Morris plot for adsorption of Safranine by CG.

transport of dyes from solution through the particle solution interface into the pores of the particle as well as the adsorption on the available surface of adsorbent were both responsible for the uptake of dye. The particle rate constants calculated from Fig. 9 are 0.2979 to 3.0361 mg/g min$^{0.5}$ (Table 2).

3.6. Adsorption isotherms

An adsorption isotherm represents the relationship existing between the amount of pollutant adsorbed and the pollutant concentration remaining in solution. Adsorption equilibrium is established when the amount of pollutant being adsorbed. At this point the equilibrium solution concentration remains constant. By plotting solid-phase concentration against liquid-phase concentration graphically it is possible to depict the equilibrium adsorption isotherm. The two most common types of isotherms are Langmuir and the Freundlich models.

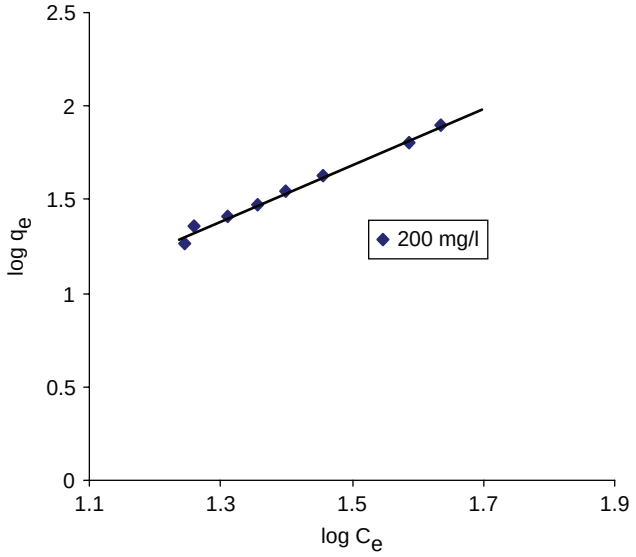

Fig. 10. Freundlich plot for adsorption of Safranine by CG.

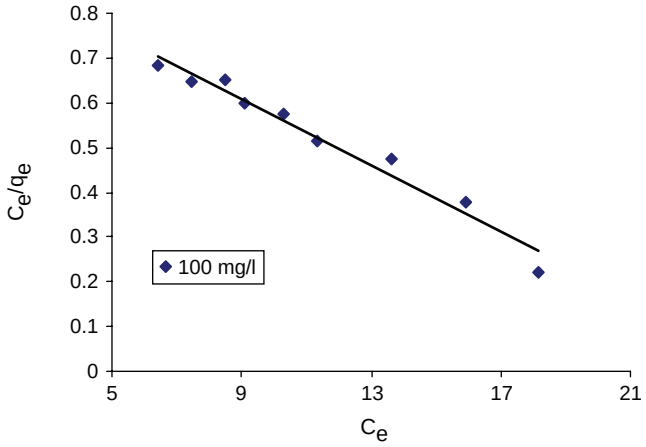

Fig. 11. Langmuir plot for adsorption of Safranine by CG.

3.6.1. Freundlich isotherm

The Freundlich isotherm is the earliest known relationship describing the sorption equation [30]. The application of the Freundlich equation suggests that sorption energy exponentially decreases on completion of the sorption centers of an adsorbent. This isotherm is an empirical equation employed to describe heterogeneous systems. The logarithmic form of Freundlich isotherm equation is

$$\log q_e = \log K_f + \frac{1}{n} \log c_e \quad (5)$$

where K_f is the equilibrium dye concentration on adsorbent (mg/g), c_e is the equilibrium dye concentration in solution (mg/l), K_f is Freundlich constant (l/g) and $1/n$ is the heterogeneity factor. The linear plot of $\log q_e$ vs. $\log c_e$ confirms the applicability of model (Fig. 10). The K_f and $1/n$ were calculated from intercept and slope of the plot and are presented in Table 3. The correlation coefficient of the graphs $r^2 \geq 0.8632$ which indicates the validity of isotherm.

3.6.2. Langmuir isotherm

The linear isotherm theory assumes monolayer coverage of adsorb ate over a homogenous adsorbent [31]. A basic assumption is that sorption takes place at specific homogenous sites within the adsorbent. Once a dye molecule occupies a site, no further adsorption can take place at that site. The Langmuir isotherm is

$$\left(c_e/q_e\right) = \left(1/ab\right) + \left(c_e/b\right) \quad (6)$$

where c_e is the concentration of dye solution (mg/l) at equilibrium. The constant '*a*' signifies the adsorption (l/mg). The linear plot of c_e/q_e vs. c_e shows that adsorption follows Langmuir isotherm (Fig. 11). Values of '*a*' and '*b*' were calculated from the slope and intercept of the linear plots and are represented in Table 3. The applicability of the Langmuir isotherm suggests the monolayer coverage of the dye on the surface of CG. The essential characteristics of the Langmuir isotherm can be expressed in terms of a dimension less constant separation factor R_L.

Separation factor $R_L = 1/(1 + bci)$ (7)

Table 3
Freundlich and Langmuir isotherm constants for adsorption of Safranine on CG for different dye concentration and adsorbent dose of 1–12 g/l at pH = 8, contact time 40 min

Dye concentration, mg/l	Freundlich coefficient				Langmuir coefficient			
	K_f, l/g	n	$1/n$	r^2	α, mg/g	β, g/l	R_L	r^2
100	3.6702	0.5404	1.8502	0.9481	26.95	0.0393	0.2028	0.9685
200	9.0531	0.5606	1.7836	0.9652	72.46	0.0128	0.2808	0.9649
300	11.0866	0.6022	1.6605	0.8632	75.19	0.0085	0.2816	0.9599
400	69.5624	0.6480	1.5432	0.9324	89.28	0.0069	0.2247	0.9622

where '*b*' is the Langmuir constant (l/mg) and c_i is the initial dye concentration (mg/l). The value of R_L indicates the shape of the isotherm to be either unfavorable ($R_L > 1$), linear ($R_L = 1$), favorable ($0 < R_L < 1$), or irreversible ($R_L = 0$). The R_L values between 0 and 1 indicate favorable adsorption. For adsorption of Safranine on CG, R_L values obtained are given in Table 3 are in the range 0.2028–0.2816, indicating that adsorption is a favorable process.

The Freundlich and Langmuir coefficients are shown in Table 3. The values of r^2 (goodness of fit criterion) computed by linear regression for both isotherm are represented in Table 3. The higher r^2 value indicates that Langmuir adsorption is most appropriate for adsorption of Safranine on CG.

4. Conclusion

The aim of this work was to explore the possible use of congress grass (CG), which is an agricultural waste available in large quantity in India, as adsorbent for the removal of Safranine from aqueous solutions. In batch mode adsorption studies, the adsorption was dependent on the solution pH, adsorbent dye concentration initial dose and contact time. The equilibrium time was 40 min. Adsorption of dye could be described by Freundlich and Langmuir isotherms. The Langmuir isotherm fit better to equilibrium data with maximum adsorption capacity 89.3 mg/g. The dimensionless separation factor R_L showed that CG can be used for removal of Safranine from aqueous solution. The adsorption kinetics followed pseudo-second-order equation indicating that chemisorptions were rate controlled step in adsorption process. The results of the intraparticle diffusion model suggested that intraparticle diffusion was not the only rate controlling step.

Thus CG is a low cost, easily available agro waste biomaterial that can be used as an alternative for more costly adsorbent used for dye removal in wastewater treatment process.

Acknowledgments

The authors are gratefully acknowledged to the Head, Centre for Nanomaterials and Quantum Systems, Department of Physics, University of Pune for SEM, XRD and EDX analysis. Authors are also thankful to Principal, GTP College Nandurbar for providing necessary laboratory facilities.

References

[1] M. Arami, N.Y. Limaee and N.M. Mahmoodi, Evaluation of the adsorption kinetics and equilibrium for the potential removal of acid dyes using a biosorbent, Chem. Eng. J., 139 (2008) 2–10.

[2] N. Barka, A. Assabbane, A. Nounach, L. Laanab and Y.A. Ichou, Removal of textile dyes from aqueous solutions by natural phosphate as a new adsorbent, Desalination, 235 (2009) 264–275.

[3] C. Galindo, P. Jacques and A. Kalt, Photo degradation of the amino benzene acid orange S2 by three advanced oxidation processes: UV/H_2O_2, UV/TiO_2 and VIS/TiO_2 comparative mechanistic and kinetic investigations, J. Photochem. Photobiol. A: Chem., 130 (2000) 35–47.

[4] B.I. Akmehmet and I. Arslan, Treatment of textile industry wastewater by enhanced photo catalytic oxidation reaction, J. Adv. Oxid. Technol., 4 (1999) 189–195.

[5] T. Parada, R. Gade, D. Fabler and K. Gunther, Quantum yield of TiO_2- photocatalysed degradation of Acid Orange 7, J. Adv. Oxid. Technol., 4 (1999) 203–208.

[6] G. Crini, Non-conventional low-cost adsorbents for removal; a review, Bioresour. Technol. 97 (2006) 1061–1085.

[7] M. Arami, N.Y. Limaee, N.M. Mahmoodi and N.S.Tabrizi, Equilibrium and kinetics studies for the adsorption of direct and acid dyes from aqueous solution by soy meal hull, J. Hazard. Mater., 135 (1–3) (2006) 171–179.

[8] N.M. Mahmoodi, M. Arami, N.Y. Limaee, K. Gharanjig and F.D. Ardejiani, Decolorization and mineralization of textile dyes at solution bulk by heterogeneous nanophotocatalysis using immobilized nanoparticles of titanium dioxide, Colloids Surf. A Physicochem. Eng. Aspects, 290 (2006) 125–131.

[9] A. Fernandes, A. Morao, M. Magrinho, A. Lopes and I. Goncalves, Electrochemical degradation of C.I. Acid Orange 7, Dyes Pigments, 61 (2004) 287–296.

[10] A. Akabari, J.C. Remigy and P. Aptel, Treatment of textile dye effluents using a polyamide based nano filtration membrane, Eng. Process., 41 (2002) 601–609.

[11] J. Wu, M.A Eiteman and S.E Law, Evaluation of membrane filtration and ozonisation processes for treatment of reactive dye wastewater, J. Environ. Eng., 124 (1998) 272–277.

[12] S.E. Bailey, T.J. Olin, R.M. Brika and D.D. Adrian, A review of potentially low cost sorbents for heavy metals, Water Res., 33 (1999) 2469–2479.

[13] M.S. El-Geundi, Adsorbents for industrial pollution control, Adsorpt. Sci. Technol., 15 (1997) 777–787.

[14] L.T. Ruey and W.W. Feng, Role of micro porosity of activated carbons on their adsorption abilities for phenols and dyes, Adsorption, 7 (2001) 65–72.

[15] V.S. Mane, I.D. Mall and V.C. Shrivastava, Use of Bagasse fly ash as an adsorbent for the removal of brilliant green dye from aqueous solution, Dyes Pigments, 73 (2007) 269–278.

[16] M. McKay, M.S. El-Geundi and M.M. Nassar, Equilibrium studies during the removal of dyestuffs from aqueous solutions using bagasse pith, Water Res., 21 (1987) 1513–1520.

[17] G.H. Sonawane and V.S. Shrivastava, Kinetics of decolorization of malachite green from aqueous medium by maize cob (Zea maize): an agricultural solid waste, Desalination, 247 (2009) 430–441.

[18] M. Ozocar and A.I. Sengil, Adsorption of metal complex dyes from aqueous solutions by pine sawdust, Bioresour. Technol., 96 (2005) 791–795.

[19] A. Haluk and B. Gulay, Adsorption of acid dyes in aqueous solutions by shells of bittim (Pistacia Khinjuk) stocks. Desalination, 196 (2006) 248–259.

[20] Y. Bulut and H. Aydin, A kinetic and thermodynamic study of methylene blue adsorption of wheat shells, Desalination, 194 (2006) 259–267.

[21] K.C. Bhattacharya and A. Sharma, Adsorption characteristics of the dye brilliant green on leaf powder, Dyes Pigments, 7 (2003) 211–272.

[22] M. Bourada, M. Lafjah, M.S.Ouali and LC. Menorval, Basic dye removal from aqueous solutions by dodecylsulphate and dodecyl benzene sulfonate intercalated hydrotalcite, J. Hazard. Mater., 153 (2008) 911–918.

[23] G. McKay, J.F. Porter and G.R. Prasad, The removal of dye colors from aqueous solutions by adsorption on low cost materials, Water Air Soil Pollution, 114 (1999) 423–438.

[24] S. Lagergren, About the theory of so-called adsorption of soluble substances. K. Sven. Vetenskapasakad Handl., 24(4) (1898) 1–39.
[25] Y.S. Ho, Sorption studies of acid dye by mixed sorbents, Adsorption, 7 (2001) 139–147.
[26] Y.S. Ho and G. McKay, Pseudo-second order model for sorption, processes, Process Biochem., 34 (1999) 451–465.
[27] Y.S. Ho, Citation review of Lagergren kinetic rate equation on adsorption reactions. Scientometrics, 59 (2004) 171–177.
[28] W.H. Cheung, Y.S. Szeto and G. McKay, Intraparticle diffusion process during acid dyes adsorption onto chitosan, Bioresource Technol., 98 (2007) 2897–2904.
[29] C.H. Wu, Adsorption of reactive dye onto carbon nanotubes equilibrium kinetics and thermodynamics, J. Hazard Mater., 144 (2007) 93–100.
[30] C. Gregorio and N.P. Harmel, Adsorption of basic blue 9 on cyclodextrin based material containing carboxylic groups, Dyes Pigments, 70 (2006) 204–211.
[31] I. Langmuir, The constitution and fundamental properties of solids and liquids, J. Am. Chem. Soc., 38 (11) (1916) 2221–2295.